RSC Advances

PAPER

View Article Online
View Journal | View Issue

Cite this: *RSC Adv.*, 2019, **9**, 42132

Intrahepatic fatty acids composition as a biomarker of NAFLD progression from steatosis to NASH by using ^{1}H-MRS

Aline Xavier, *[ab] Flavia Zacconi,[cde] Constanza Gainza,[f] Daniel Cabrera,[gh] Marco Arrese,[g] Sergio Uribe,[abi] Carlos Sing-Long[abfj] and Marcelo E. Andia[abi]

Non-alcoholic fatty liver disease (NAFLD) is the most common liver disease in the world and it is becoming one of the most frequent cause of liver transplantation. Unfortunately, the only available method that can reliably determine the stage of this disease is liver biopsy, however, it is invasive and risky for patients. The purpose of this study is to investigate changes in the intracellular composition of the liver fatty acids during the progression of the NAFLD in a mouse model fed with Western diet, with the aim of identify non-invasive biomarkers of NAFLD progression based in ^{1}H-MRS. Our results showed that the intracellular liver fatty acid composition changes as NAFLD progresses from simple steatosis to steatohepatitis (NASH). Using principal component analysis with a clustering method, it was possible to identify the three most relevant clinical groups: normal, steatosis and NASH by using ^{1}H-MRS. These results showed a good agreement with the results obtained by GC-MS and histology. Our results suggest that it would be possible to detect the progression of simple steatosis to NASH using ^{1}H-MRS, that has the potential to be used routinely in clinical application for screening high-risk patients.

Received 29th October 2019
Accepted 10th December 2019

DOI: 10.1039/c9ra08914d

rsc.li/rsc-advances

Introduction

Non-alcoholic fatty liver disease (NAFLD) is characterized by the accumulation of intracellular fatty acids in the liver in the absence of excessive alcohol consumption. The spectrum of this disease starts with a simple steatosis; it may progress to non-alcoholic steatohepatitis (NASH) with different degrees of inflammation, and with or without fibrosis; and ultimately cirrhosis and hepatocellular carcinoma.[1] NAFLD is strongly associate with obesity and metabolic syndrome, which are the most common non-transmissible chronic diseases in Western countries.[1,2]

Research performed in 2015 with a sample of 8 515 431 patients from 22 countries showed that 25% of the total population in the world suffers from NAFLD.[3] According to statistics, about 30–40% of people with steatosis develop NASH. Moreover, 10–30% of them develop cirrhosis, which could progress to hepatocellular carcinoma.[4]

Currently, there are no specific biomarkers that can predict this "bad progression" of NAFLD. Most of the current available diagnosis methods mainly focus on estimating the total amount of fat stored in the liver using ultrasound (US), computed tomography (CT) or magnetic resonance imaging (MRI). However, these methods have some drawbacks: US does not work properly in obese patients, CT uses ionizing radiation and none of these methods can recognize either inflammation or early stages of fibrosis. In addition, it is necessary to detect the disease in NASH stages while the disease is reversible.[5] Therefore, the only method that can reliably determine the stage of this disease is a biopsy with a histological evaluation, however, it is invasive and risky for patients.[6–8]

In an attempt to develop biomarkers correlated with the progression of the disease, previous studies have characterized the fatty acids (FA) stored in the intracellular lipids in the liver by using gas chromatography with mass spectrometer (GC-MS), and they have identified some changes in the FA profile when comparing healthy livers, livers with steatosis, and livers with steatohepatitis.[9–12] Araya *et al.* (2004)[12] found a decrease in polyunsaturated fatty acids (PUFA), while the saturated fatty acids (SFA) and the monounsaturated fatty acids (MUFA) had no

[a]*Biomedical Imaging Center, Pontificia Universidad Católica de Chile, Chile. E-mail: acarvalhodasilva@uc.cl*
[b]*Millennium Nucleus for Cardiovascular Magnetic Resonance, Chile*
[c]*Faculty of Chemistry and Pharmacy, Pontificia Universidad Católica de Chile, Chile*
[d]*Research Center for Nanotechnology and Advanced Materials CIEN-UC, Pontificia Univesidad Católica de Chile, Chile*
[e]*Institute for Biological and Medical Engineering, Schools of Engineering, Medicine and Biological Sciences, Pontificia Universidad Católica de Chile, Chile*
[f]*Institute for Mathematical and Computational Engineering, Pontificia Universidad Católica de Chile, Chile*
[g]*Gastroenterology Department, School of Medicine, Pontificia Universidad Católica de Chile, Chile*
[h]*Department of Chemical and Biological Sciences, Universidad Bernardo O'Higgins, Chile*
[i]*Radiology Department, School of Medicine, Pontificia Universidad Católica de Chile, Chile*
[j]*Millennium Nucleus Center for the Discovery of Structures in Complex Data, Chile*

significant changes between healthy patients and patients with steatosis. This study also found a decrease of the long chain polyunsaturated fatty acids between healthy patients and patients with steatosis, and between patients with steatosis and patients with steatohepatitis. Additionally, the same conclusion was found by Puri *et al.* (2007).[11]

Although the analysis of the lipid composition opens an interesting field for the diagnosis of fatty liver progression, it still requires a biopsy, so its routine use is limited. On the other hand, magnetic resonance spectroscopy (MRS) provides a non-invasive technique that allows to determine the structure of organic substances.[7] The idea of defining a classifier using MRS emerges due to the need to find a way to replace biopsy with a non-invasive method that can classify NAFLD based on the composition of different fatty acids stored in the liver.

Previous studies have shown that it is possible to associate the results of MRS with those obtained from GC-MS. Unfortunately, those studies considered only fatty acids with 14, 16 and 18 carbons and not fatty acids with long chain, which seems to have a big relevance in the NAFLD progression.[13–16] Furthermore, studies that emphasize the importance of fatty acids on the liver have analyzed it *in vivo* with MRS but have not correlated their results with the true amount of fatty acids as no biopsy was performed.[17–20]

The purpose of this study is to investigate and compare the intracellular composition of the liver fatty acids using histology, GC-MS, 9.4T ^{1}H-MRS during the progression of NAFLD in a mice model fed with Western diet, with the aim of identifying non-invasive biomarkers of NAFLD progression to NASH.

Subjects and methods

All experiments were approved by the Scientific Ethics Committee for the care of animals and the environment of the Pontificia Universidad Católica de Chile (number: 170614002).

We fed a group of C57BL/6 male mice with Western diet (AIN76A, Test Diet) for 4 weeks ($n = 6$), 10 weeks ($n = 6$) and 24 weeks ($n = 6$). The Western diet has 4.49 kilocalories per gram, and the calories come from: fat (40%), protein (15.8%), and carbohydrate (44.2%). We also fed a group ($n = 6$) with a chow diet (500l*, Labdiet) with 3.36 kilocalories per gram, and the calories come from: fat (13.4%), protein (30%), and carbohydrate (57%). The Western diet is a model of "Western fast food" diet characterized by high calories, high cholesterol and high fructose content.[21]

At the end of the diet intervention, the mice were anesthetized with ketamine/xylosine, and the livers were harvested. A portion of the liver was used for histology analysis. The remaining liver was divided into two portions that were analyzed independently. We extracted the intracellular FA using a protocol adapted by Folch *et al.*,[22] proceeded by an esterification process to obtain fatty acids methyl esters (FAME) since they are more stable (do not form hydrogen bridges). It's important to comment that the quantity of FA is the same as FAME. Finally, those FAME were analyzed using a 9.4 T MRS and GC-MS.

Previous studies were performed and allowed the conclusion that 300 mg of liver was required since, after the extraction in healthy mice, we obtained 5 mg of FAME and that is the minimum amount of sample required to perform a ^{1}H MRS with enough SNR. For the GC-MS, 2 mg of FAME is enough.[23]

Gas chromatography with mass spectrometer

FAME were analyzed by using gas chromatography with mass spectrometer (PerkinElmer, Clarus 680) equipped with HP-Innowax capillary column (length 25 meters, 0.2 mm internal diameter, 0.2 mm film). Additional configuration of GC-MS is found in Table 1. Data register was in SCAN mode and peak integration was obtained by the TurboMass Training 2016 PRO software.

FAME were identified by comparing retention times to known standards and by matching them up with the mass spectra from NIST library (National Institute of Standards and Technology, USA).

The mass of each FAME (in μg) was calculated according to the integration area of corresponding peak and the relation with the integration area of the internal standard (C19 : 0) added to the sample (50 μg). Fatty acids composition was defined as the percentage of individual fatty acids in respect of its total.

Magnetic resonance spectroscopy

The ^{1}H MRS spectra of the FAME were obtained in a Bruker Avance spectrometer operating at 9.4 Tesla with the acquisition protocol Zg30 (30 degrees in z axis).

We took a known value in mg of FAME from each sample and added 700 μl of $CDCl_3$ that has a small proportion of tetramethylsilane (TMS) as an internal reference. This mixture was introduced into a 5 mm diameter tube. The spectra acquisition was made with Topspin V3.0 and the parameters were: spectral width 8012.820 Hz, relaxation delay 1 s, number of scans 16, acquisition time 2.045 s, flip angle 30° to avoid T1 relaxation effects and total acquisition time 48.72 s (number of scans × [time between pulses + acquisition time]). The experiment was conducted at 25 °C. The spectra were analyzed using MestreNova Version 10.0. First, the spectra were centered (TMS in 0 ppm); then we calculated the area under the curve (AUC) of all seven peaks corresponding to fatty acids and finally, we normalized the AUC by the total amount of fatty acids. The fatty acids peaks used were: methyl terminal protons (–C**H**$_3$, approximately 0.9 ppm); bulk methylene protons (–C**H**$_2$–, approximately 1.3 ppm); β-methylene protons (COO–C**H**$_2$–CH$_2$–, approximately 1.6 ppm); allylic protons (–C**H**$_2$–CH=CH-, approximately 2.0 ppm) α-methylene protons (COO–C**H**$_2$–CH$_2$–, approximately 2.2 ppm); diallylic protons (=CH–C**H**$_2$–CH=, approximately 2.8 ppm) and olefinic internal protons (–C**H**=C**H**–, approximately 5.3 ppm).

Histology

Liver sections from mice livers were routinely fixed in 10% of formalin and embedded in paraffin. Then 5 μm tissue sections were stained with hematoxylin/eosin, oil red and Picrosirius Red, as described previously.[24] Whole slide imaging was

Table 1 Gas-chromatography-mass spectrometer (Clarus 680 PerkinElmer) configuration

Injector temp.	Oven ramp	Sample injection	Electron impact
220 °C	150 °C × 1 min 15 °C min^{-1} to 200 °C 200 °C × 5 min 12 °C min^{-1} to 260 °C	Split mode (1 : 20) helium at 1 ml min^{-1} (constant flow)	Ionization potential of 70 eV

obtained using the Aperio Digital Pathology Slide Scanner (Leica Biosystems) allowing us to study the entire left lateral lobe. Histopathological analyses were performed by a blinded pathologist starting from three full cross-sectional slides obtained from distal, medial, and proximal regions derived from the left lateral lobe. The blinded trained pathologist utilized the NAFLD Activity Score (NAS) by using the method proposed by Kleiner *et al.*[25]

The score of steatoses vary between 0 and 3, the score of ballooning vary between 0 and 2, the score of inflammation vary between 0 and 3, and the score of fibrosis vary between 0 and 4. The NAS is the sum of steatosis, ballooning and inflammation scores. It can vary between 0 and 8. A NAS score less than 3 means no NASH, while a score higher than 4 means NASH. Scores of 3 or 4 means indeterminate.

Correlation between GC-MS and MRS

The MRS allows us to determine the structure of an organic substance. The spectrum shows the signals in a graph of frequency (ppm) *versus* intensity in arbitrary units. Each set of chemically equivalent protons originates a signal in such a way that the number of signals in a spectrum indicates the amount of different kinds of protons in a substance. The chemical shift is a measure of how far away the signal is from the reference signal of tetramethylsilane (TMS). The greater the displacement with respect to the TMS (0 ppm) is, the closer the proton is to an environment where there is an electronegative group.[26]

The GC is the gold standard to characterize fatty acids. The mixture containing all the fatty acids methyl esters is introduced in a GC-MS where it is warmed, and the fatty acids start to separate from each other by their volatility and polarity.[27]

There are many types of FA in the liver of a human being. All of them generate just seven peaks corresponding to the chemical equivalent protons. Fig. 1 shows an example of a FAME with 18 carbons and 2 double bonds in the signal of the MR spectroscopy.

Therefore, MRS does not detect the quantity of the fatty acids directly, but it is possible to assume that, if we have a change in fatty acids profile, we will have a change in the metabolites detected by MRS.

Statistical analyses

All statistical analyses were performed using Prism 6 (GraphPad Software Inc, La Jolla, CA). All graphs were plotted as mean ± standard deviation or boxplot. To compare between 3 or more groups, the ANOVA test was performed followed by a Bonferroni *post-hoc* test. A *P*-value < 0.05 was considered to indicate statistical significance.

Principal component analysis and clustering method

Even though mice are fed with the same amount of diet for a fixed period, the disease may progress differently in each mouse. In order to identify changes in fatty acids and metabolites, we have used principal component analysis (PCA) to visualize the stage of the disease in each mouse, and a clustering method to group the mice according to their GC-MS and MRS measurements.

PCA is a data analysis technique that is used to represent a large set of data samples with a reduced set of features that explain most of the variability in the original set. These features, called principal components, are determined by finding linear combinations of the data samples that explain the largest variability in the dataset. Therefore, the first principal component corresponds to the direction of maximum possible variance, whereas the second explains the maximum remaining variance and so on.[28] By considering a small number of principal components, we can visualize the data and determine if there is a natural distribution of the measurements performed on each mouse that correlates to their disease progression.

To determine if the distribution of GC-MS and ^{1}H-MRS data has itself some structure from which we can infer the presence or progression of the disease, an agglomerative hierarchical clustering method was applied. Agglomerative hierarchical clustering is a "bottom-up" approach; each data point is initially considered to be a cluster, and data points are grouped together at each step according to some criterion. At the end of the procedure we obtain several potential groupings of the data, with a decreasing number of clusters.[28] For our analysis, the data points are grouped according to their Euclidean distance and Ward's linkage function.[29] This choice promotes that at

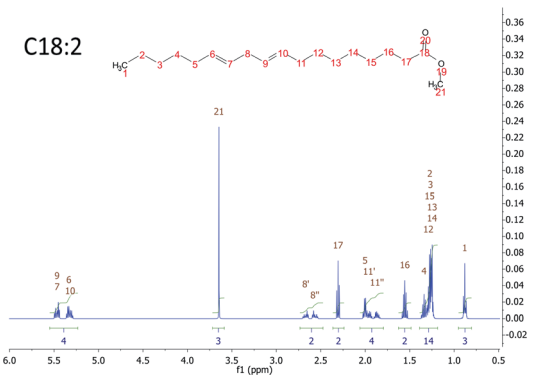

Fig. 1 MRS simulation of a FAME with 18 carbons and 2 double bonds. The proton chemically equivalent are shown in numbers.

Table 2 Mice age, weight and the percentage of FAME in the liver for each group. The first group was fed with a chow diet, the second, third and fourth group was fed with a Western diet for 4, 10 and 24 weeks, respectively

Mice group	Mice age (weeks)	Mice weight (g)	Liver weight (g)	Weight of FAME/total liver sample, %
Chow-diet (control)	16	26.63 ± 1.33	1.22 ± 0.07	3.07 ± 0.65
Western diet for 4 weeks	16	28.27 ± 2.76	1.14 ± 0.08	5.84 ± 2.11
Western diet for 10 weeks	22	36.23 ± 6.24	1.61 ± 0.56	12.68 ± 4.28
Western diet for 24 weeks	36	46.23 ± 2.12	3.32 ± 0.48	23.62 ± 2.54

each step, among all possible choices, pairs of clusters are merged in order to minimize the variation within the resulting cluster with respect to all other possible choices.

Results

Mice fed with Western diet increased their weight and accumulated fat in the liver. Table 2 shows the mice weight, liver weight and the total liver FAME content (mass of FAME/total liver sample, %) for each group at 4 time points: 0, 4, 10 and 24 weeks since diet intervention. By comparing the total amount of fatty acid in two portions of the same liver (that were analyzed independently before averaging), we identified a maximum difference of 5%.

Histology

Fig. 2 shows the results of histology for each group. Besides that, the average score and the range of steatosis, ballooning, inflammation and fibrosis for each group is shown below the image. The NAFLD activity score (NAS) for each group was, in average, 0 (zero) for control group with chow diet, 0.8 for the group of mice with Western diet for 4 weeks, 4.4 for the group of mice with Western diet during 10 weeks and 7.8 for the group of mice with Western diet during 24 weeks.

Fig. 3 shows a boxplot with individual values of the NAS score. The control group, mice fed with Western diet for 4 weeks and two mice fed with Western diet for 10 weeks have no NASH, while the mice fed with Western diet for 24 weeks and four mice fed with Western diet for 10 weeks have NASH.

Gas chromatography with mass spectrometer

We identified 12 main fatty acids using the CG-MS, however, 5 of them had less than 1% of participation, therefore, we only considered 7 FA for the analysis (C16 : 0, C18 : 0, C16 : 1, C18 : 1, C18 : 2, C20 : 4, C22 : 6). Two of the FA changed significantly between all the groups (control, 4 weeks-diet, 10 weeks-diet and 24 weeks-diet) corresponding to the progression

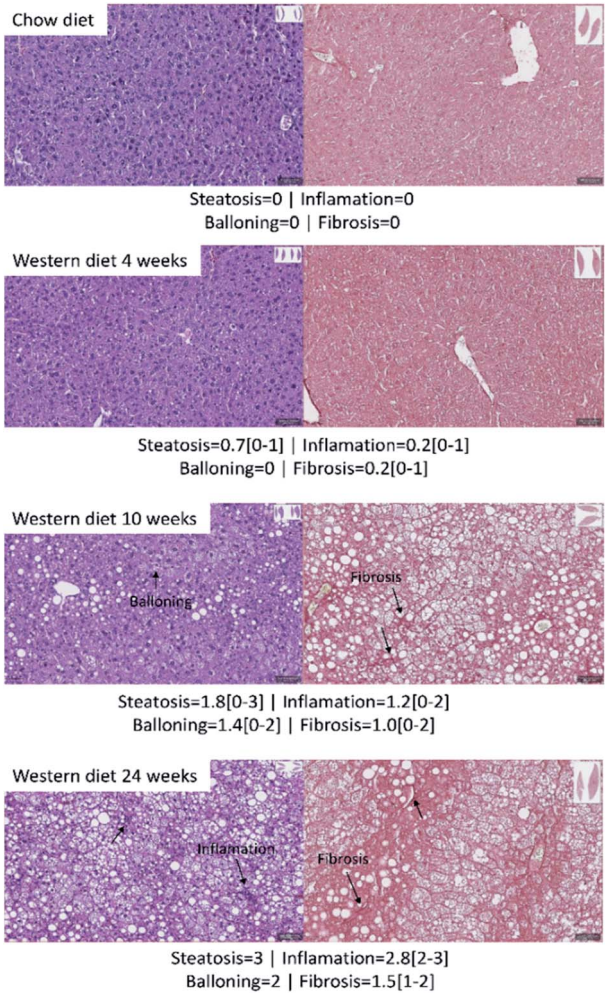

Fig. 2 Hepatic histology results with hematoxylin/eosin (left) and picrosirius red (right). The average score and the range of steatosis, ballooning, inflammation and fibrosis for each group is shown below the image.

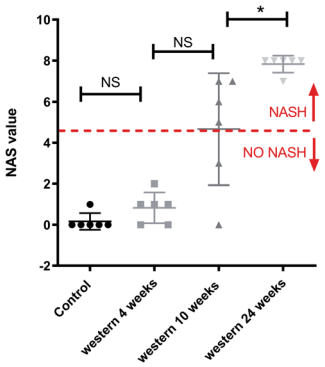

Fig. 3 Boxplot of NAS score and value for each mouse individually. NAS value varies between 0 and 8: a value bigger or equal to 5 means that the mouse has NASH.*$p < 0.05$ (significant difference between groups) and NS (no significant difference between groups).

of NAFLD: C18 : 1 increased, while C18 : 2 decreased. Other two FA (C16 : 1 and, C22 : 6) changed significantly between 3 of the 4 groups, C16 : 1 increased, while C22 : 6 decreased (Fig. 4). Additionally, by comparing the composition of the fatty acids in two portions of the same liver, we identified a maximum difference of 2.5%, most of them less than 1%.

All the FA can be grouped into three main categories: saturated fatty acids (SFA), monounsaturated fatty acids (MUFA) and polyunsaturated fatty acids (PUFA). The SFA have no double bonds (*i.e.*, C14 : 0, C15 : 0, C16 : 0, C18 : 0), while the MUFA have one double bond (*i.e.*, C16 : 1, C18 : 1) and the PUFA have two or more double bonds (*i.e.*, C18 : 2, C18 : 3, C20 : 3, C20 : 4, C20 : 5, C22 : 6).

Fig. 5 shows that PUFA liver content decreased with the progression of the disease from 40.5% in control group to 4.5% at 24 weeks ($P_{ANOVA} < 0.001$). In contrast, MUFA liver content increased from 26.8% in control group to 67.8% at 24 weeks ($P_{ANOVA} < 0.001$), while SFA remain constant.

Magnetic resonance spectroscopy

We have identified seven metabolite peaks in the MRS spectra that correspond to the FA and the peak of methyl ester (3.6 ppm). Fig. 6 shows a visual comparison between a representative spectrum of one control group mouse and the spectrum of a mouse fed Western diet for 24 weeks. Five peaks (terminal methyl, bulk methylene, allylic, diallylic and olefinic) showed significant differences with the progression of the disease (Fig. 7). However, the terminal methyl group should not change since this peak is present in all FA, with the same quantity of protons. The alfa and beta methylene should be present in all FA with the same number of protons; therefore, we shouldn't expect any significant differences.

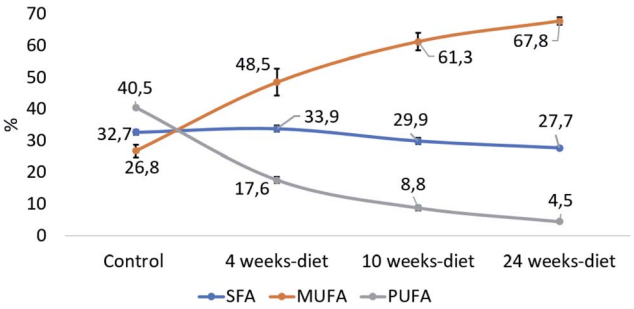

Fig. 5 The relative contribution of each group of fatty acids: saturated fatty acids (SFA: C14 : 0, C15 : 0, C16 : 0, C18 : 0), monounsaturated fatty acids (MUFA, C16 : 1, C18 : 1) and polyunsaturated fatty acids (PUFA, C18 : 2, C18 : 3, C20 : 3, C20 : 4, C20 : 5 C22 : 6).

Principal component analysis

The principal components for the FA composition measured with GC-MS and metabolites identified in the ^{1}H-MRS were computed separately; and the data projected onto the space generated by their corresponding first two principal components (Fig. 8a and b). In this 2-dimensional representation it is possible to identify changes in the GC-MS measurements as the time of diet intervention increases and the disease progresses (Fig. 8a). In particular, the control group and the mice fed for 24 weeks are well-separated. This behavior is replicated for the ^{1}H-MRS measurements (Fig. 8b) indicating the potential for ^{1}H-MRS to be used both as a biomarker for the progression of the disease and as a surrogate for GC-MS.

The three groups that can be visually identified show a rough correlation with the number of weeks each mouse has been fed (Fig. 8a and b). Interestingly, the group of mice fed for 10 weeks

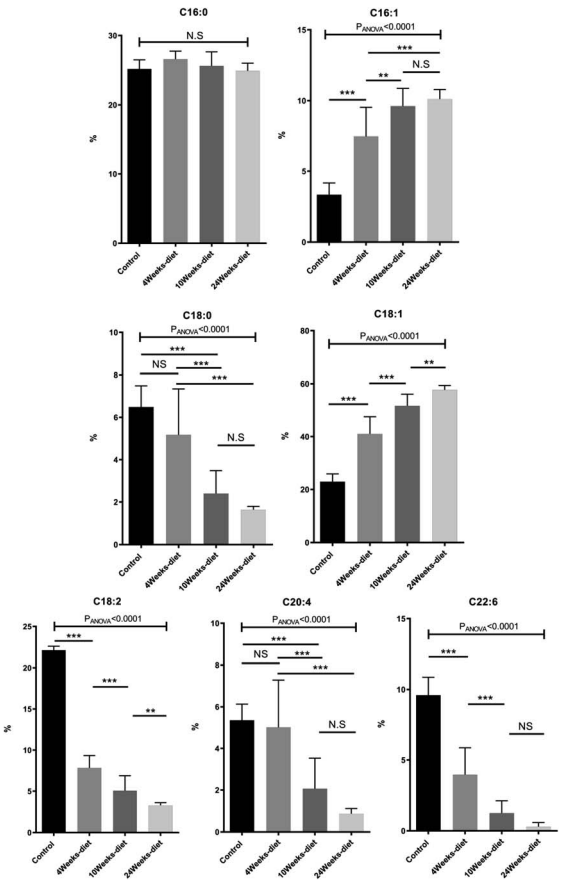

Fig. 4 Change in fatty acids composition measured with GC-MS (mean ± SD) for the four different groups of mice (control or chow diet, 4 weeks of Western diet, 10 weeks of Western diet and 24 weeks of Western diet). *$p < 0.05$, **$p < 0.01$, ***$p < 0.001$ (significant difference between groups) and NS (no significant difference between groups).

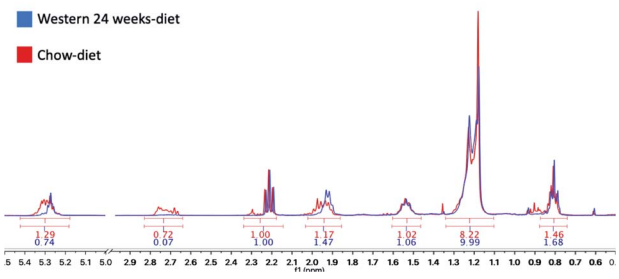

Fig. 6 Areas under the curve (AUC) calculated with MestreNova V10.0. In red, the results of a control mouse with a chow-diet and in blue, a mouse with a Western diet for 24 weeks.

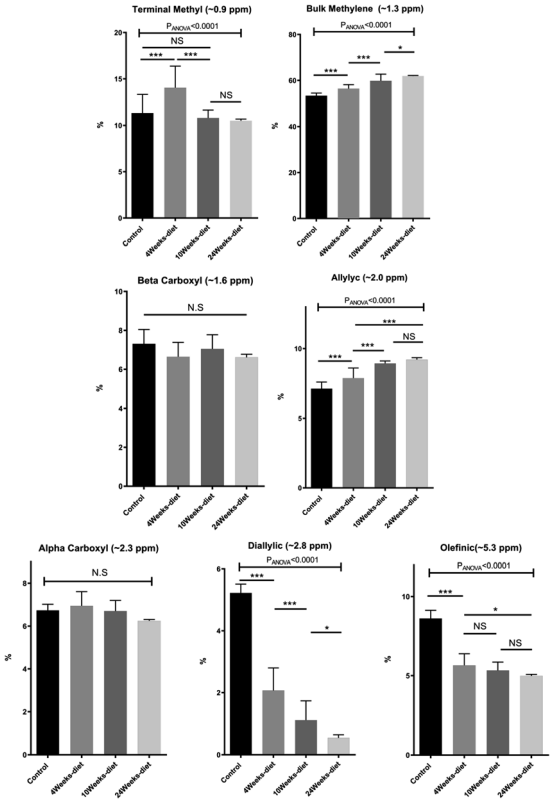

Fig. 7 Change in the AUC of the 7 peaks measured in the 1H-MRS (mean ± SD) for the four different groups of mice (control or chow diet, 4 weeks of Western diet, 10 weeks of Western diet and 24 weeks of Western diet). *$p < 0.05$, **$p < 0.01$, ***$p < 0.001$ (significant differences between groups) and NS (no significant difference between groups).

has been split in two, with some of them grouped with mice fed for 4 weeks, and the rest grouped with mice fed for 24 weeks. Those grouped with the mice fed for 4 weeks are those with no NASH whereas those grouped with the mice fed for 24 weeks are precisely those that have NASH (Fig. 3).

We used agglomerative hierarchical clustering to group both the GC-MS and 1H-MRS data (Fig. 8c and d). Interestly, the clusters obtained correspond to three stages of NAFLD: the first one with a low NAS score, normal; the second one, with an intermedium NAS score, low to medium steatosis; and the third one with high NAS score with inflammation and early stages of fibrosis.

Furthermore, the mouse whose result is at the top of the GC-MS graph (Fig. 8a) was grouped as a control mouse, even though it was fed with Western diet for 4 weeks. However, its NAS value was 0. Fig. 9 shows the mean of NAS score for each the cluster identified (control, No NASH, NASH).

Discussion

We have analysed the effects of a diet intervention with a fast food-like model (*i.e.*, Western diet) in mice for 24 weeks. During the progression of the disease, the mice consecutively develop steatosis, steatohepatitis and liver fibrosis, with a progressive

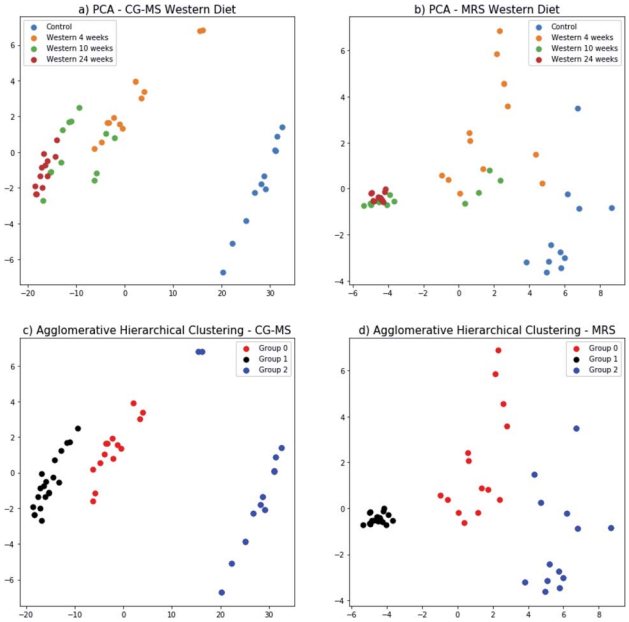

Fig. 8 Principal component analysis of GC-MS results (a) and MRS results (b) for all the groups of mice (control, 4 weeks Western diet, 10 weeks Western diet, and 24 weeks Western diet). Agglomerative hierarchical clustering method to cluster the data of GC-MS (c) and MRS (d). *x*-axis id the principal component 1 and *y*-axis is the principal component 2.

increase in the NAS score. Simultaneously, Western diet produced numerous changes in liver fatty acids composition, which could provide new evidence to understand the progression of the disease and identify biomarkers to predict the progression of steatosis and NASH.

GC-MS analysis showed that the fat in the liver is composed of, at least, 12 different fatty acids, which have different evolution during the NAFLD progression. Besides that, the analysis

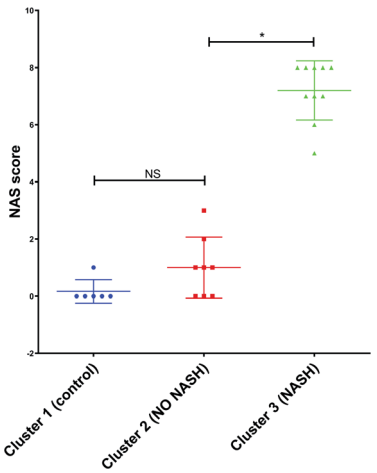

Fig. 9 NAS score for each cluster found by PCA with the data from GC-MS and MRS. *$p < 0.05$ (significant difference between groups) and NS (no significant difference between groups).

identifies a pattern of fatty acids composition during NAFLD progression: although the total amount of fatty acids increased during the NAFLD progression, not all the fatty acids progressed in the same way. The PUFA decreased, while the MUFA increased and the SFA remained the same during the progression of the disease. Similar results were found by Levant *et al.* (2013) in mice with a high-fat diet for 8 weeks.[30] The decrease in the PUFA can be explained since the arachidonic (C20 : 4); eicosapentaenoic acid (20 : 5) and docosahexaenoic acids (C22 : 6) are precursors for a variety of anti- and pro-inflammatory mediators.[31,32]

MRS analysis found all the seven peaks related to fatty acids. The diallylic peak (2.8 ppm), corresponding to FA with two or more double bonds, also decreased in good agreement with the PUFA results found by CG-MS. The olefinic (5.3 ppm), allylic (2.0 ppm) and bulk methylene (1.3 ppm) peaks are somehow related to this change in PUFA and MUFA, because they are related to double bonds.

As mentioned by Leporq *et al.* (2014), who used only theoretical values calculated from oil mass composition for validation, one of the limitations of their work was not to have the gas chromatography analysis as gold standard to characterize those FA.[33] Opposite to this, our study overcomes this limitation with the GC-MS analysis.

Our results, as evidenced by PCA, showed that the liver fatty acid composition changes as NAFLD progresses. In addition, by using agglomerative hierarchical clustering it was possible to identify the 3 most relevant clinical groups: normal, steatosis and NASH. In essence, the NAS score of the entire population was reproduced by clustering the GC-MS data in three groups. In addition, applying the same analysis to the ^{1}H-MRS data shows it is possible to identify the same 3 groups using *ex-vivo* MRS, which provide some evidence that the proposed methodology could be used *in vivo* and non-invasive, however further studies has to be done to prove this hypothesis.

Some limitations of our studies are related to the possibility that our results may vary if the mice were fed with different diets, although we have used the diet most like human diet.[34,35] However, this limitation might explain differences in the NAFLD progression among patients, in which some of them evolve to NASH and cirrhosis, whereas others remain in the early stages of NAFLD for a long time.

Additionally, the MRS acquisition was performed only over the extracted liver fatty acids, so that it is now necessary to validate our results with *in vivo* whole liver MRS acquisition. The transition to an *in vivo* measurement has some challenges since it may account with a series of extra parameters like respiratory and cardiac motion, presence of water component, the correlation between acquisition time, NSA, voxel size and SNR to assure the comfort of the patient, but also the spectra quality.

Preliminary results showed that it would be possible to identify the same 7 peaks in human and mice livers *in vivo* at 7.0 T (ref. 36) and 9.4 T (ref. 37), respectively (Fig. 10). Although the 7.0 T is not available for clinical use yet, research could be made in this equipment by benefitting from its good spectral resolution to validate the method.

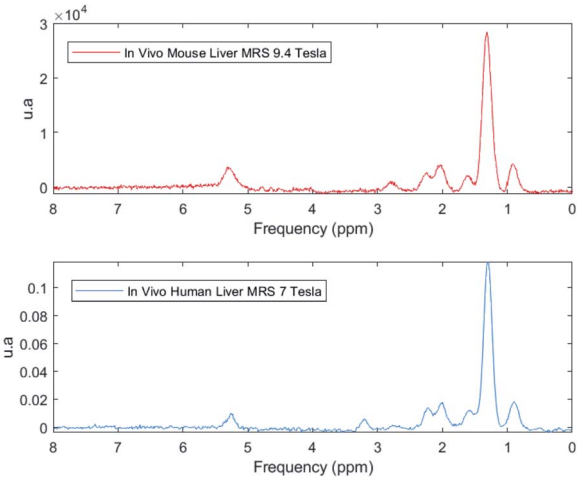

Fig. 10 *In vivo* MR spectra from a 9.4 Tesla in a mouse (red) and 7 Tesla in human (blue) showing that it is possible to identify all the seven peaks correspondent to the fat spectrum in the liver.

Conclusions

To conclude, our study compares different stages of the NAFLD disease induced by a Western diet. The differences in the FA composition found by GC-MS, which is also reflected in the MR spectrum, could have clinical potential for monitoring NAFLD progression from steatosis to NASH in a non-invasive way.

Conflicts of interest

There are no conflicts to declare.

Acknowledgements

This publication has received funding from Millennium Science Initiative of the Ministry of Economy, Development and Tourism, grant Nucleus for Cardiovascular Magnetic Resonance and grant Millennium Nucleus Center for Discovery of Structures in Complex Data, FONDECYT 1180525, 11171001 and 1191145 to MA, DC and MA respectively. CONICYT-PCHA/Doctorado Nacional/2016-21160835. CSL was partially funded by FONDECYT 11160728. FZ is grateful to FONDEQUIP EQM120021 and EQM150020 from Pontificia Universidad Católica de Chile.

References

1 S. L. Friedman, B. A. Neuschwander-Tetri, M. Rinella and A. J. Sanyal, *Nat. Med.*, 2018, **24**(7), 908–922.
2 R. Wiliams and S. D. Taylor-Robinson, *Clinical Dilemmas in Non-Alcoholic Fatty Liver Disease*, 1st edn, 2016.
3 Z. M. Younossi, A. B. Koenig, D. Abdelatif, Y. Fazel, L. Henry and M. Wymer, *Hepatology*, 2016, **64**(1), 73–84.
4 M. G. Neumann and L. B. Cohem, *Can. J. Gastroenterol. Hepatol.*, 2014, **28**(11), 607–618.

5 R. J. Perry, D. Zhang, X. M. Zhang, J. L Boyer and G. I. Shulman, *Science*, 2015, **347**, 1253–1256.
6 M. Ahmed M, *World J. Hepatol.*, 2015, **7**(11), 1450–1459.
7 Z. Permutt, T.-A. Le, M. R. Peterson, E. Seki, D. A. Brenner, C. Sirlin and R. Loomba, *Aliment. Pharmacol. Ther.*, 2012, **36**(1), 22–29.
8 S. B. Reeder, I. Cruite, G. Hamilton and C. B. Sirlin, *J. Magn. Reson. Imaging*, 2011, **34**(4), 729–749.
9 K. Yamada, E. Mizukoshi, H. Sunagozaka, K. Arai, T. Yamashita, Y. Takeshita, H. Misu, T. Takamura, S. Kitamura, Y. Zen, Y. Nakanuma, M. Honda and S. Kaneko, *Liver Int.*, 2015, **35**(2), 582–590.
10 G. Guo and X. Zhang, *Lipids in healthy and disease*, 2011, vol. 10, p. 234.
11 P. Puri, R. A. Baillie, M. M. Wiest, F. Mirshahi, J. Choudhury, O. Cheung, C. Sargeant, M. J. Contos and A. J. Sanyal, *Hepatology*, 2007, **46**(4), 1081–1090.
12 J. Araya, R. Rodrigo, L. A. Videla, L. Thielemannt, M. Orellana, P. Pettinelli and J. Poniachik, *Clin. Sci.*, 2004, **106**, 635–643.
13 G. Knote and J. Kenar, *Eur. J. Lipid Sci. Technol.*, 2004, **106**(2), 88–96.
14 M. D. Guillen and A. Ruiz, *J. Sci. Food Agric.*, 2003, **83**(4), 338–346.
15 Y. Miyake, K. Yokomizo and N. Matsuzaki, *J. Am. Oil Chem. Soc.*, 1998, **75**, 15–19.
16 J. Ren, I. Dimitrov, A. D. Sherry and C. R. Malloy, *J. Lipid Res.*, 2008, **49**, 2055–2062.
17 G. Hamilton, T. Yokoo, M. Bydder, I. Cruite, M. E. Schroeder, C. B. Sirlin and M. S. Middleton, *NMR Biomed.*, 2011, **24**, 784–790.
18 R. Longo, P. Pollesello, C. Ricci, F. Masutti, B. J. Kvam, L. Bercich, L. S. Croce, P. Grigolato, S. Paoletti, B. de Bernard, C. Tiribelli and L. D. Palma, *J. Magn. Reson. Imaging*, 1995, **5**, 281–285.
19 N. A. Johnson, D. W. Walton, T. Sachinwalla, C. H. Thompson, K. Smith, P. A. Ruell, S. R. Stannard and J. George, *Hepatology*, 2008, **47**, 1513–1523.
20 Y. Lee, H.-J. Jee, H. Noh, G.-H. Kang, J. Park, J. Cho and H. Kim, *Magn. Reson. Med.*, 2013, **70**(3), 620–629.
21 A. Krishnan, T. S. Abdullah, T. Mounajjed, S. Hartono, A. McConico, T. White, N. LeBrasseur, I. Lanza, S. Nair, G. Gores and M. Charlton, *Am. J. Physiol.: Gastrointest. Liver Physiol.*, 2017, **312**, G666–G680.
22 J. Folch, M. Lees and G. H. Sloane Stanley, *J. Biol. Chem.*, 1957, **226**(1), 497–509.
23 A. Xavier, F. Zacconi, D. Cabrera, K. Fuenzalida and M. E. Andia, *IFMBE Proceedings*, 2019, vol. 70, (1), pp. 51–56.
24 D. Cabrera, A. Wree, D. Povero, N. Solís, A. Hernandez, M. Pizarro, H. Moshage, J. Torres, A. E. Feldstein, C. Cabello-Verrugio, E. Brandan, F. Barrera, J. P. Arab and M. Arrese, *Sci. Rep.*, 2017, **7**(1), 3491.
25 D. E. Kleiner, E. M. Brunt, M. Van Natta, C. Behling, M. J. Contos, O. W. Cummings, L. D. Ferrell, Y. C. Liu, M. S. Torbenson, A. Unalp-Arida, M. Yeh, A. J. McCulloughJ and A. J. Sanyal, *Hepatology*, 2005, **41**(6), 1313–1321.
26 P. B. Yurkanis, *Química orgânica*, 5th edn, 2008.
27 A. Di Giulio and A. Bonamore, *Globins and Other Nitric Oxide-Reactive Proteins Part A*, 2008, pp. 239–253.
28 G. James, D. Witten, T. Hastie and R. Tibshirani, *An Introduction to Statistical Learning*, 2013, ch. 6 and 10.
29 J. H. Ward Jr, *J. Am. Stat. Assoc.*, 1963, **58**(301), 236–244.
30 B. Levant, M. K. Ozias, B. L. Guilford and D. E. Wright, Streptozotocin-induced diabetes partially attenuates the effects of a high-fat diet on liver and brain fatty acid compo-sition in mice, *Lipids*, 2013, **48**, 939–948.
31 N. G. Bazan, *Brain Pathol.*, 2005, **15**, 159–166.
32 G. Bannenberg, M. Arita and C. N. Serhan, *Sci. World J.*, 2007, **7**, 1440–1462.
33 B. Leporq, S. A. Lambert, M. Ronot, V. Vilgrain and B. E. Van Beers, *NMR Biomed.*, 2014, **27**, 1211–1221.
34 L. H. Tetri, M. Basaranoglu, E. M. Brunt, L. M Yerian and B. A. Neuschwander-Tetri, *Am. J. Physiol.: Gastrointest. Liver Physiol.*, 2008, **295**, G987–G995.
35 L. Longato, *Fibrog. Tissue Repair*, 2013, **6**, 14.
36 A. Filmer, C. A. Castro, A. Xavier, P. R. Luijten, D. W. Klomp and J. J. Prompers, *ISMRM proceeding*, 2019, p. 4232.
37 A. Xavier, F. Zacconi, T. Eykyn, B. Plaza, A. Phinikaridou and M. E. Andia. *MAGMA: Book of abstract ESMRMB*, 2019, vol. 32, (1), p. S55.